

Electronic Supplementary Information

Layered Double Hydroxide-based Nanozyme for NO-boost Multi-enzyme Dynamic Therapy with Tumor Specificity

Xueting Yang,^{#1,2} Xin Cao,^{#1,2} Ye Fu,⁴ Jun Lu,² Xiaotong Ma,¹ Ran Li,^{1,2} Shanyue Guan,^{*1} Shuyun Zhou,¹ and Xiaozhong Qu^{*3}

1 Key Laboratory of Photochemical Conversion and Optoelectronic Materials, Technical Institute of Physics and Chemistry, Chinese Academy of Sciences, Beijing, 100190, China.

2 State Key Laboratory of Chemical Resource Engineering, Beijing University of Chemical Technology, Beijing 100029, China

3 College of Materials Science and Opto-Electronic Technology, University of Chinese Academy of Sciences, Beijing 100049, China

4 College of Chemistry and Materials Engineering, Beijing Technology and Business University, Beijing, 100048, China.

[#] These authors contributed equally to this work.

Experimental Section

Reagents and Chemicals

Zincnitrate Hexahydrate ($\text{Zn}(\text{NO}_3)_2 \cdot 6\text{H}_2\text{O}$), Manganese (II) nitrate hydrate ($\text{Mn}(\text{NO}_3)_3 \cdot \text{H}_2\text{O}$), Aluminum nitrate nonahydrate ($\text{Al}(\text{NO}_3)_3 \cdot 9\text{H}_2\text{O}$), sodium hydroxide (NaOH), sodium nitrate (NaNO_3), Ferrous sulfate (FeSO_4), glutathione (GSH), 3,3',5,5'-tetramethylbenzidine (TMB), and indocyanine green dye (ICG) were purchased from Sigma-Aldrich. L(+)-Arginine, methyl blue (MB), 5,5'-dithiobis (2-nitrobenzoic acid) (DTNB) was purchased from Shanghai Aladdin Biochemical Technology Co., Ltd. Calceinacetoxymethyl ester (Calcein-AM), propidium iodide (PI), 4',6-diamidino-2-phenylindole, dilactate (DAPI), 2,7 Dichlorodihydrofluorescein diacetate (DCFH-DA) were purchased from Sigma-Aldrich Co. Ltd (St. Louis, MO, USA). Dulbecco's modified Eagles medium (DMEM), 0.25% trypsin-EDTA, penicillin/streptomycin, Fetal bovine serum (FBS), Phosphate buffered saline (PBS) were purchased from Beijing Solarbio Science and Technology Company. The 5,5-dimethyl-1-pyrroline N-oxide (DMPO) and cell counting Kit 8 (CCK-8) were purchased from Dojindo China Co., Ltd. All of the cells were obtained from the Institute of Basic Medical Sciences Chinese Academy of Medical Sciences. All other reagents and solvents were of analytical purity and used without further purification. The DI water was used during all experiments.

Characterization

XRD patterns were carried out by using a Bruker DAVINCI D8 ADVANCE diffractometer. Sample morphologies were characterized using a JEOL-2100F TEM. The size and thickness of samples were determined by AFM (Veeco). FT-IR spectra were recorded using a Perkin Elmer GX spectrophotometer. UV-Vis absorbance spectra were collected on a Beijing PGENERAL TU-1901 spectrometer. The compositions of samples were determined by inductively coupled plasma atomic emission spectroscopy (ICP-AES), ESR spectra were collected on a JES-FA200 at 110K.

NO generation

The NO-generated performance of LDHzyme was investigated by using commercial Griess reagent. Briefly, the NO standard curve can be collected by detecting the absorbance at 546 nm, which was the NO standard liquid reacted with N-(1-naphthyl) ethylenediamine dihydrochloride. Then, the NO release of LDHzyme after reacted with H₂O₂ (100 μM) at pH 5.5 was explored by using the Griess method.¹ We further evaluated the LDHzyme concentration-dependent NO release under mimic TME, which shows regularly enhance with the increase of LDHzyme concentration.

Enzyme-like activity of LDHzyme

The ROS-generated ability of LDHzyme was investigated by chromogenic reaction including TMB oxidation and MB degradation.^{2,3} TMB can be oxidized by ROS and then form a blue color with absorbance at 650 nm. Different concentrations (100, 120, 140, 160, 180 μM) of TMB and LDHzyme (50 μg/mL) were incubated with pH 5.5 buffer solution containing 100 μM H₂O₂ for 5 min. OXD-like activity can be investigated by a similiar method, while the difference is that the reaction system didn't include H₂O₂. The absorbance of the reaction system was then recorded by UV-vis spectrophotometer.

Similarly, MB can be oxidized by ROS with the maximum absorption at 650 nm declines. The MB (10 μM) and LDHzyme (50 μg/mL) were mixed with H₂O₂ in pH 5.5 buffer solution and incubated for a specified interval. The UV-vis absorption of the reaction system was recorded at different time points.

GSH depleting of LDHzyme

The GSH depletion ability of LDHzyme was explored spectrophotometrically using Ellman's reagent based on DTMB chromogenic reaction.⁴ The amount of GSH can be quantified by detecting the absorbance at 405 nm. Briefly, GSH (200 μM) and DTNB (200 μM) were co-incubated with LDHzyme (50 μg/mL) or Mn-LDH (50 μg/mL) in a pH 5.5 buffer solution for 5 min. The supernatants were extracted and the absorption intensity at 405 nm was measured to quantify the amount of GSH.

ESR measurement of ROS generation

DMPO was used as a trapping agent of ROS to detect the free radical generation ability of LDHzyme. Three sets of conditions were studied: (1) free L-Arg; (2) L-Arg + H₂O₂; (3) Mn-LDH + H₂O₂; (4) LDHzyme + H₂O₂. The reaction suspension was mixed with DMPO (10 μM) and the ROS signal was detected with ESR.

Cell culture

HeLa, HepG2, and LO2 cells were separately incubated in a growth medium (DMEM and RPMI1640 with glutamine respectively) supplemented with 10% v/v fetal bovine serum (FBS) and 1% v/v penicillin-streptomycin solution. The cells were cultured at 37 °C in a humidified atmosphere with 5% CO₂ in an incubator (Thermo Scientific).

Cell internalization of LDHzyme

The cellular uptake efficiency was explored by CLSM. Typically, HeLa cells were incubated in culture dishes at a density of 1×10^5 cells per well and grown in DMEM at 37 °C in humidified 5% CO₂ atmosphere for 24 h. Then, the culture media were replaced with fresh DMEM containing Cy5.5-labelled LDHzyme (50 g/mL), and the cells were further cultured at 37 °C for 1h and 3h, respectively. The free Cy 5.5 treated cell were served as the control group. Thereafter, the cells were washed with PBS three times and stained with mito-tracker and lyso-tracker under the dark for another 15 min. After washing with PBS, the cells were observed by CLSM to monitor the fluorescence signal of the probes with an excitation wavelength of 405 nm, 488 nm, and 641 nm, respectively.

***In vitro* ROS generation of LDHzyme-based enzyme-like activity**

The DCFH-DA was used to investigate the ROS generation of LDHzyme, which can be oxidized to fluorescent DCFH.⁵ HeLa cells were plated in culture dishes at a density of 1×10^5 cells per well and grown in DMEM at 37 °C for 24 h. Thereafter, the cells were treated with 1 mL fresh DMEM containing H₂O₂, LDHzyme, L-Arg + H₂O₂ (pH 6.5), Mn-LDH + H₂O₂ (pH 6.5), and LDHzyme + H₂O₂ (pH 6.5) for 4 h, respectively. Then,

the cells were washed with PBS and stained with DCFH-DA for another 15 min. After removal of the DMEM containing probes, the fluorescence intensity of cells was collected by CLSM with an excitation wavelength of 488 nm. The untreated cells were set as the control group.

***In vivo* distribution study**

All animal experiments were performed in compliance with the relevant laws and institutional guidelines of the University of Chinese Academy of Sciences (UCAS) and approved by the Institutional Animal Care & Welfare Committee of UCAS. Male Balb/c mice (Balb/c-nu, ~25 g) were purchased from Beijing HFK Bioscience CO., LTD. The HeLa tumor-bearing mice were achieved by subcutaneously injected with around 10^6 HeLa cells into the left foreleg.

When the tumor volume of mice exceeded 100 mm^3 , free ICG, ICG-Mn-LDH, and ICG-LDHzyme were intravenously injected into the HeLa tumor-bearing mice. The fluorescence images of mice were monitored at scheduled time points by using *in vivo* imaging system. The average fluorescence intensities from ICG in tumor were assessed to investigate the *in vivo* biodistribution of Mn-LDH and LDHzyme.

***In vivo* tumor suppression of LDHzyme**

When the tumor volume of mice exceeded $80\text{-}100 \text{ mm}^3$, 20 mice were randomly divided into four groups randomly, with 5 mice in each group, and injected with: i) PBS, ii) L-Arg, iii) Mn-LDH, and iv) LDHzyme solution (5 mg/kg) every 4 days. During 20 days of corresponding treatment, the body weights and tumor sizes were recorded every other day. The volume of tumors was calculated according to the following equation:

$$\text{Tumor volume (V)} = 0.5 \times L \times W^2$$

where L represents the long diameter, while the W indicates the short diameter, respectively. The tumor volume of PBS group in Figure S14 was calculated to 766.51 mm^3 . The relative tumor volume (V/V_0) is obtained by normalizing to the initial volume (V_0). The mice were sacrificed to collect their major organs (heart, liver, spleen, lung, and kidney) and tumors in 20 d post-treatment for TUNEL, H&E, and Ki-67 staining assay.

Statistical analysis

Data were presented as mean \pm standard deviation (SD) through at least three experiments. Origin ProPorable was used for data statistics and statistical significance calculation. Microsoft Excel 2019 was used for tumor size and mice weight analysis. Significant differences between two means were analyzed according to two-sided Student's t-test with $*p < 0.05$, $**p < 0.01$, $***p < 0.001$.

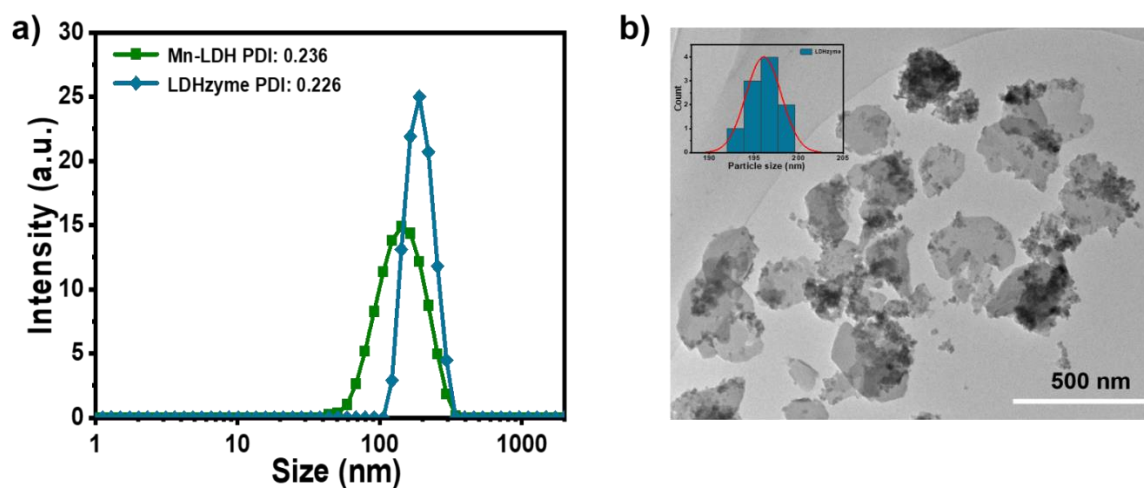


Figure S1. a) DLS results of Mn-LDH and LDHzyme. b) HRTEM images of LDHzyme.

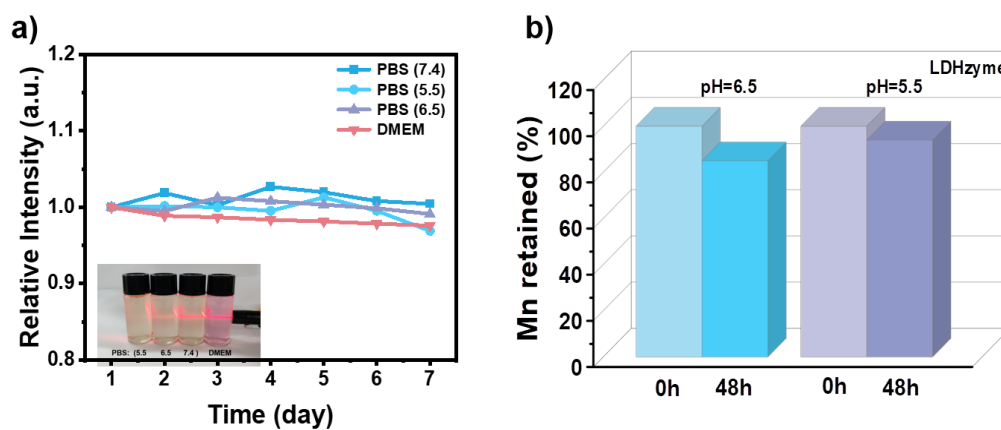


Figure S2. a) The stability of LDHzyme under various conditions: i) PBS5.5; ii) PBS6.5; iii) PBS7.4 and iii) DMEM. b) The stability of Mn of LDHzyme under various conditions (pH=5.5, pH=6.5). The Mn retained on LDHzyme were measured by inductively coupled plasma atomic emission spectroscopy (ICP-AES).

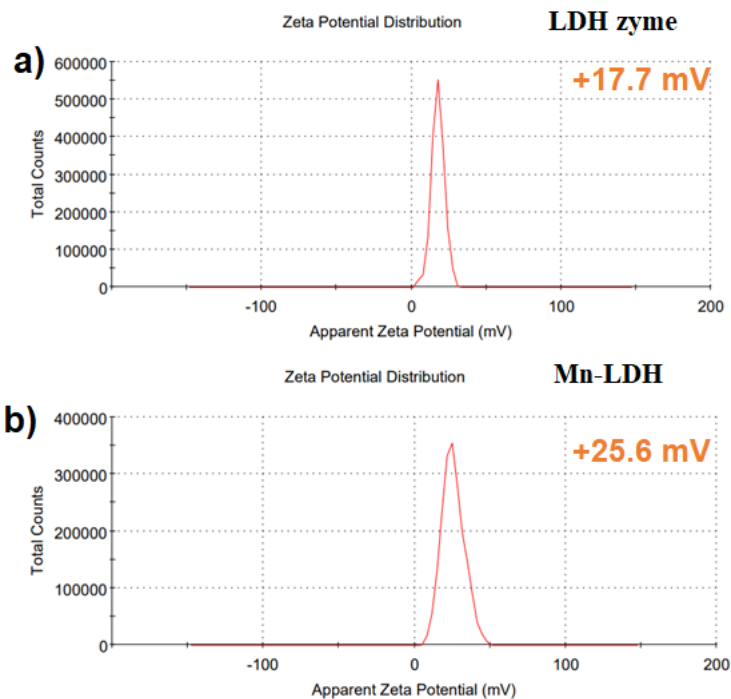


Figure S3. Zeta Potential of a) LDHzyme and b) Mn-LDH, respectively.

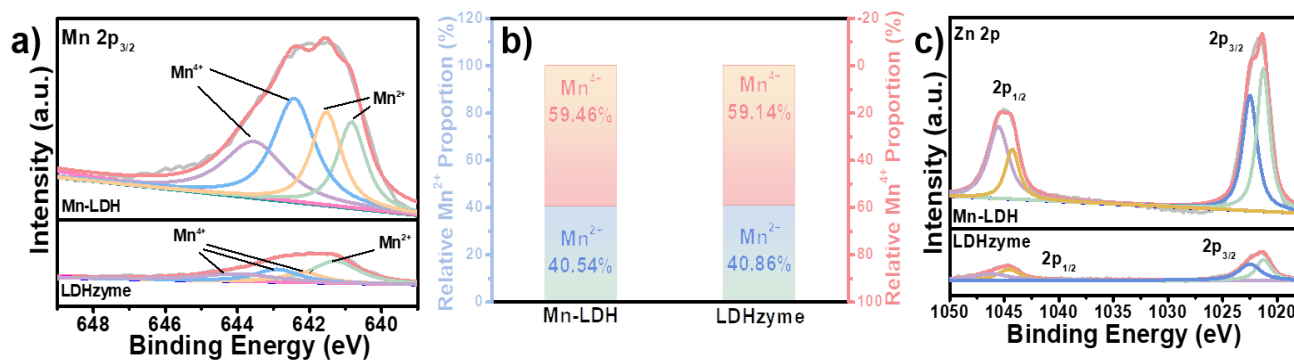


Figure S4. a) Mn 2p XPS spectra of Mn-LDH and LDHzyme. b) The relative Mn²⁺ and Mn⁴⁺ proportion of Mn-LDH and LDHzyme, respectively. c) Zn 2p XPS spectra of Mn-LDH and LDHzyme

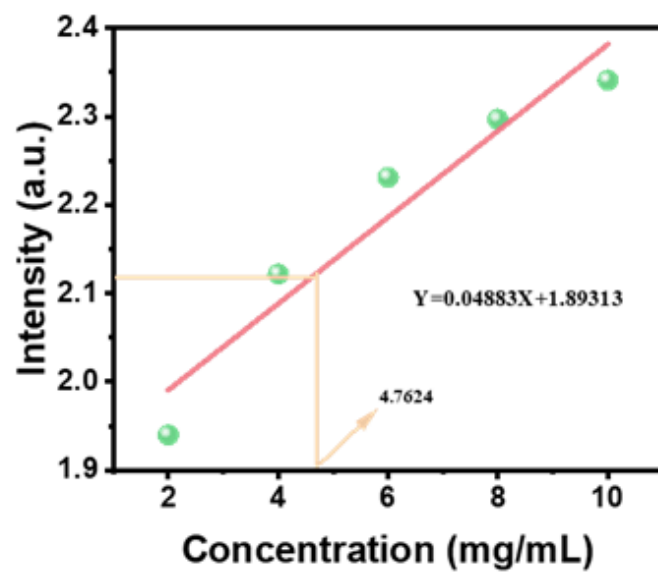


Figure S5. The loading efficiency of L-Arg.

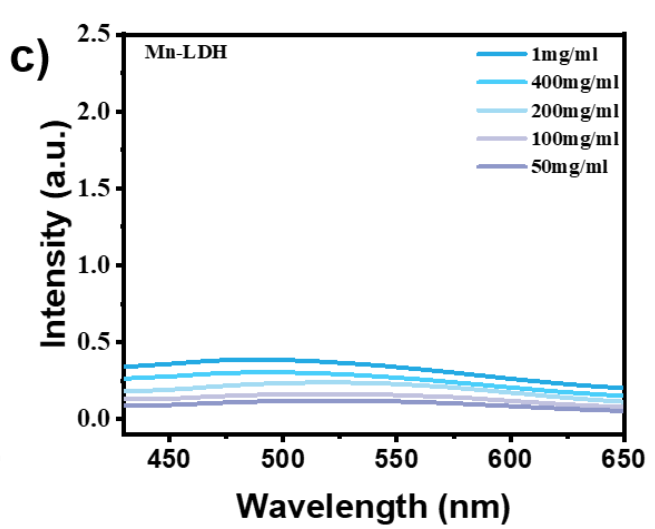
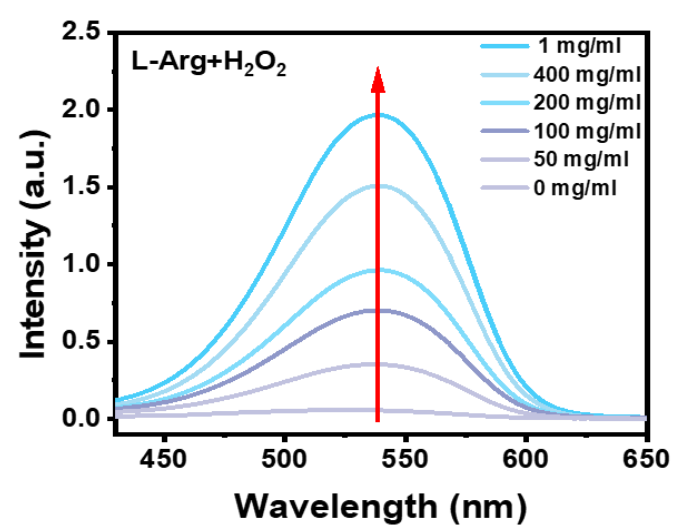
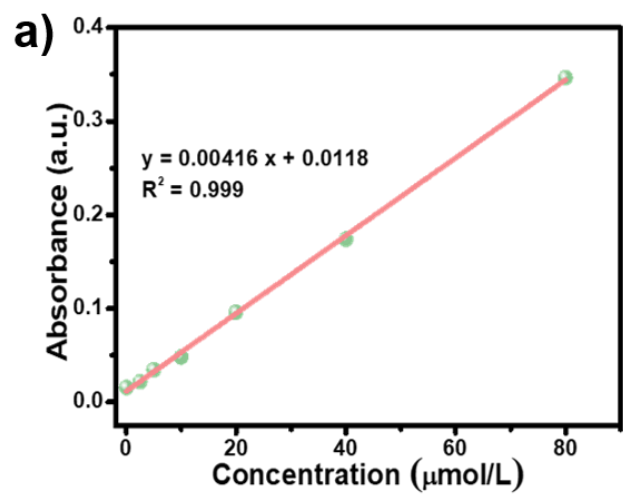


Figure S6. a) The standard curve of NO release with Griess method. b) NO release of L-Arg and c) Mn-LDH.

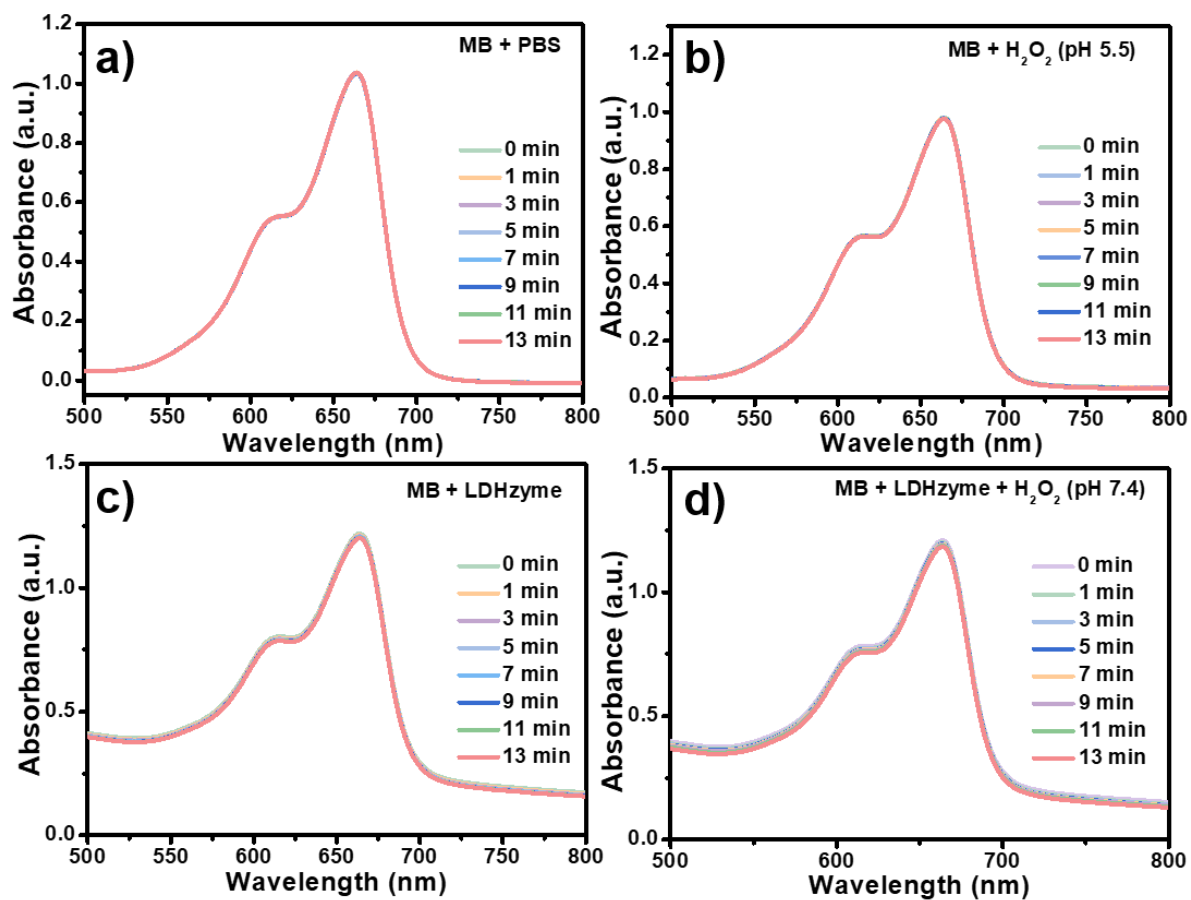


Figure S7. The MB degradation with different treatment: a) PBS, b) H₂O₂ (pH5.5), c) LDHzyme, and d) LDHzyme + H₂O₂ (pH 7.4) at different time points.

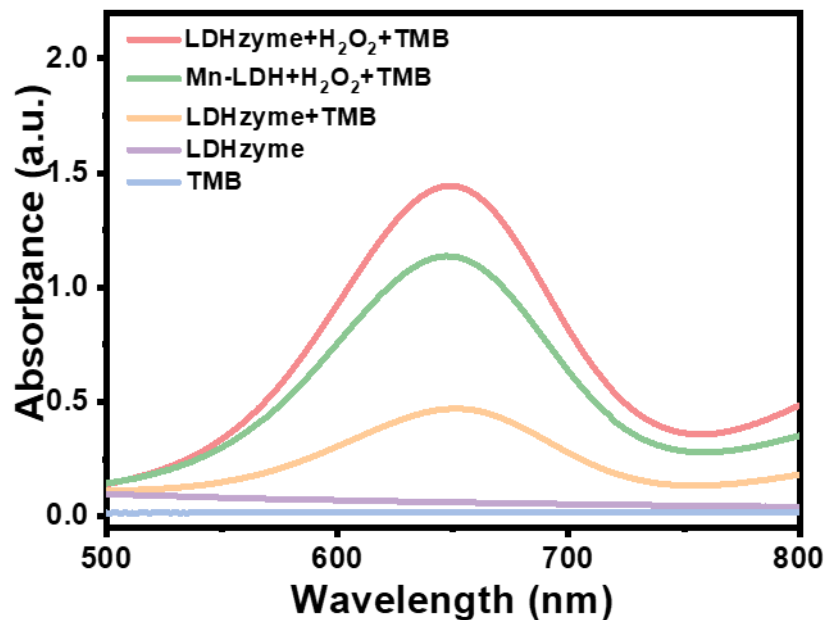


Figure S8. UV-vis absorption spectra of TMB after being treated with Mn-LDH and LDHzyme under different microenvironments.

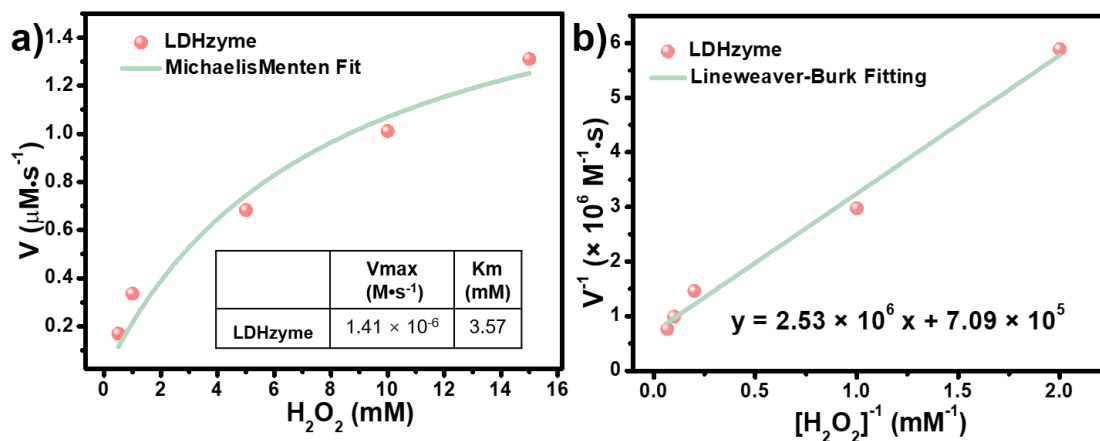


Figure S9. Michaelis–Menten steady-state kinetics of LDHzyme. a) Michaelis–Menten kinetics and b) Lineweaver–Burk plotting of LDHzyme upon the addition of varied concentrations of H₂O₂.

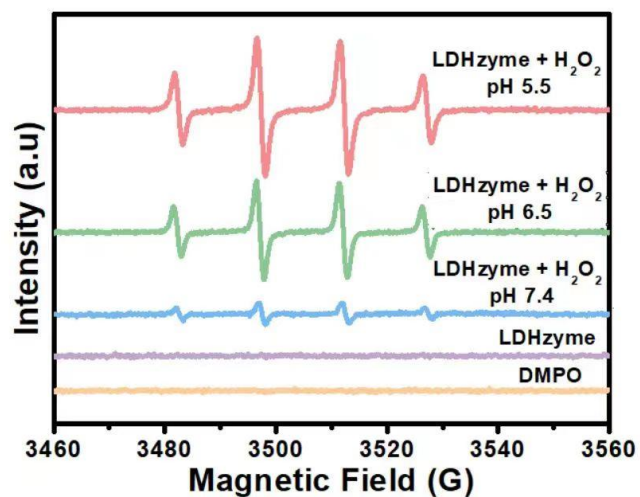


Figure S10. ESR spectra of ROS generation with different treatments: LDHzyme, LDHzyme + H₂O₂ with various pH values.

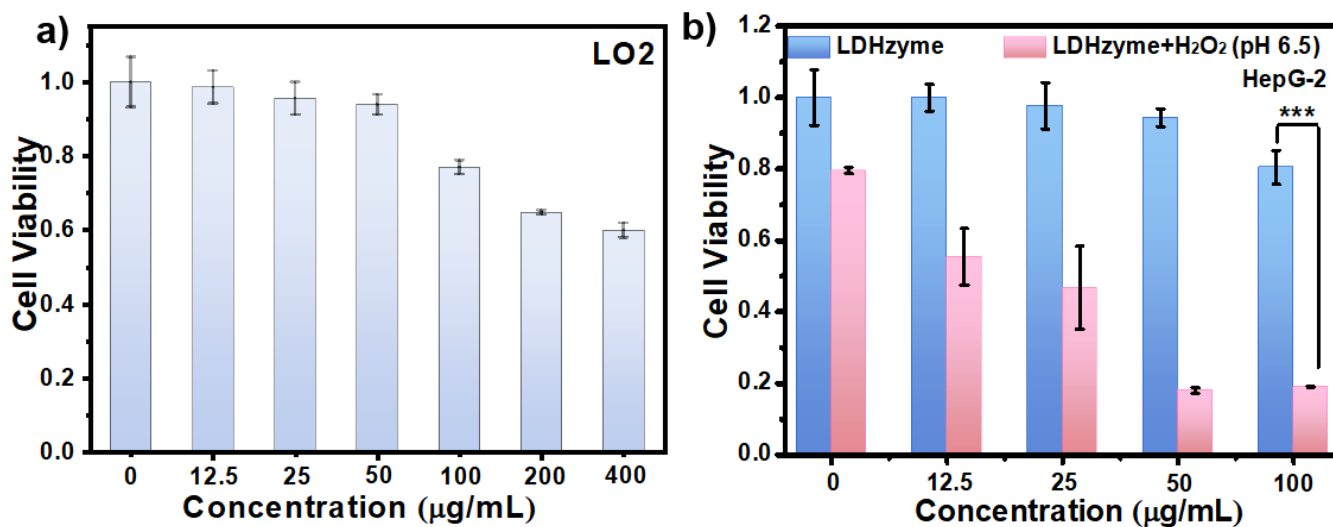


Figure S11. a) Cell viability of LO2 cells treated with the different concentrations of LDHzyme. (b). Cell viability of HepG-2 cells after treated with LDHzyme and LDHzyme + H₂O₂ at pH 6.5.

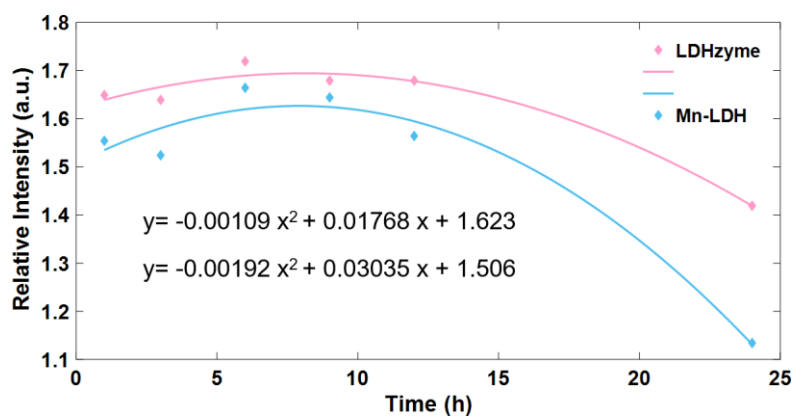


Figure S12. The function fitting diagram of the fluorescence intensity versus time.

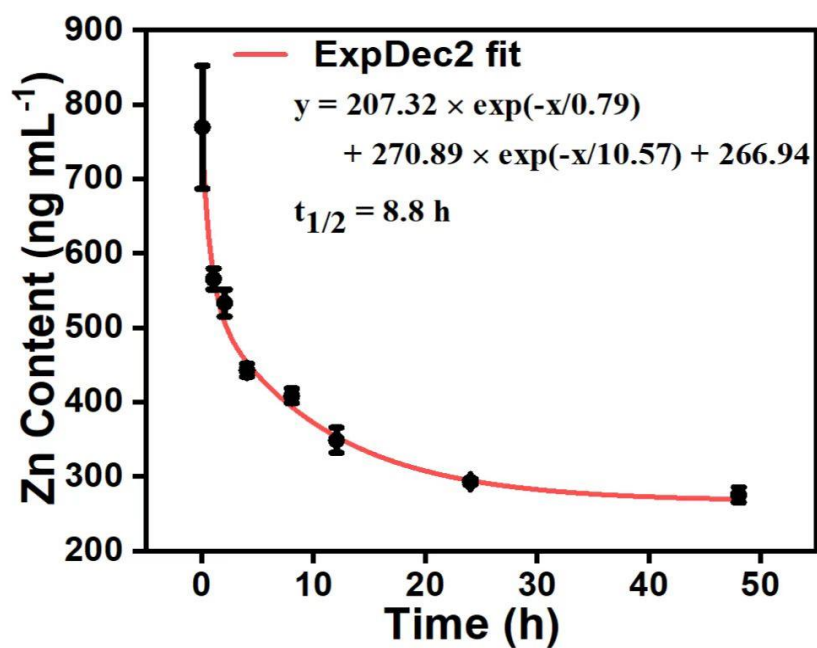


Figure S13. Zn content in the blood of mice injected with LDHzyme.

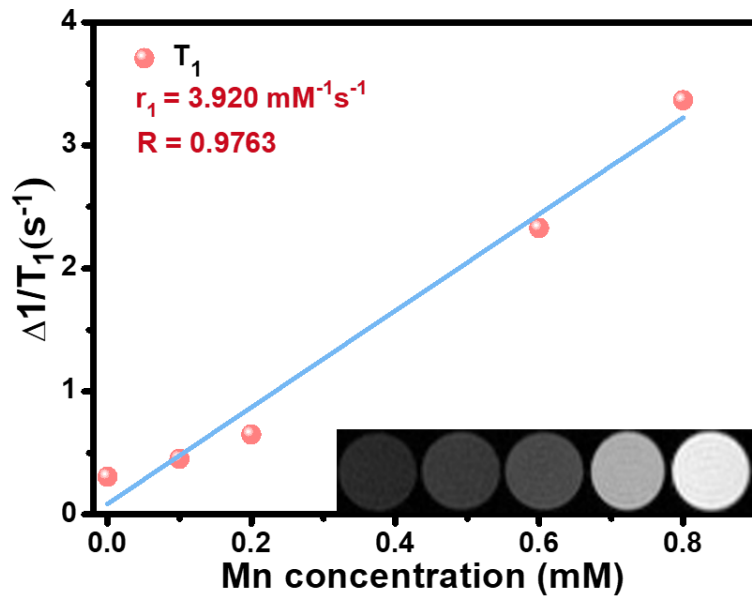


Figure S14. T_1 relaxation rate of the LDHzyme at different Mn concentrations. Inset: the corresponding T_1 -weighted MR images in aqueous solution.

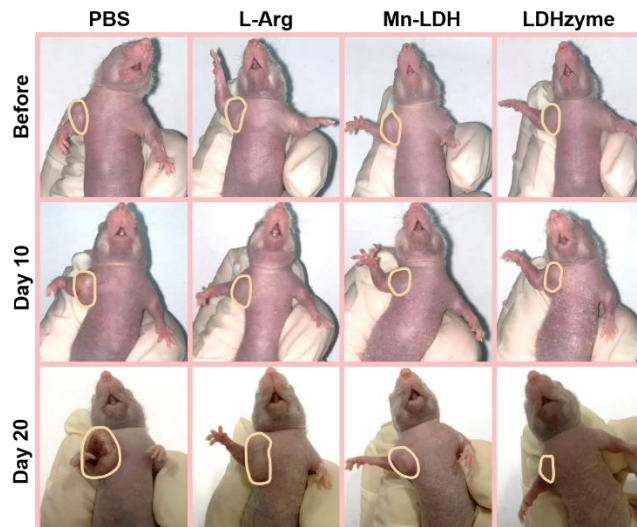


Figure S15. Representative photographs of the HeLa tumor-bearing mice after being treated with PBS, L-Arg, Mn-LDH, and LDHzyme on day 0, 10, and 20, respectively.

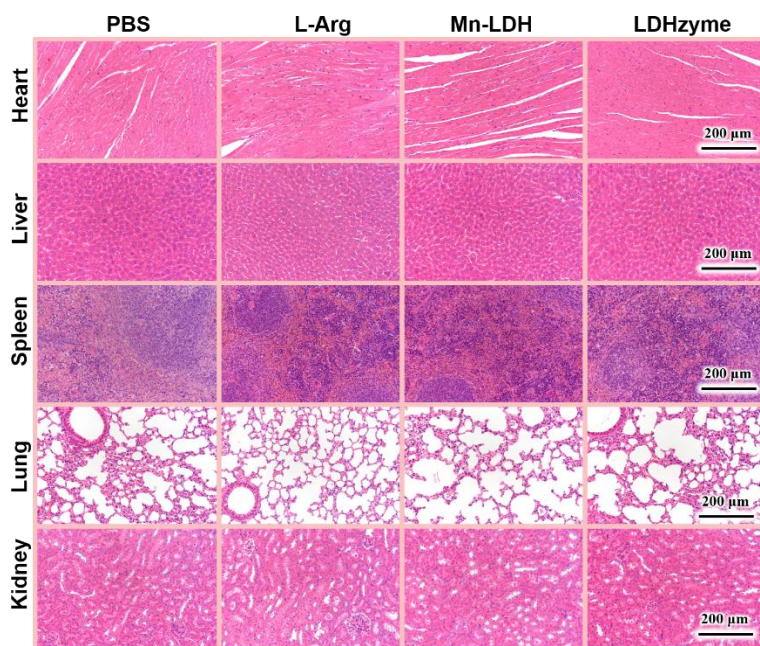


Figure S16. H&E staining of main organs (heart, liver, spleen, lung, and kidney) of mice after treated with different formula.

Table S1. The calculated V_{\max} and V_m from published research.

Sample	V_{\max} ($M \cdot s^{-1}$)	K_m (M)	Reference
CFMS-PVP	2.74×10^{-8}	0.46×10^{-3}	<i>Adv. Sci.</i> 2020 , 7, 2000272
Pd SAzyme	1.51×10^{-7}	1.79×10^{-3}	<i>Angew. Chem. Int. Ed.</i> 2021 , 60, 12971
Mn/PSAE	1.6×10^{-7}	0.09×10^{-3}	<i>Angew. Chem. Int. Ed.</i> 2021 , 60, 2 – 11
DMSN- Fe_3O_4	1.996×10^{-8}	10.10×10^{-3}	<i>Adv. Sci.</i> 2019 , 6, 1801733
GOD/CuFe-LDHs	1.69×10^{-7}	0.132×10^{-3}	<i>Chem. Sci.</i> , 2021 , 12, 2594–2603
PDA/ Fe_3O_4	2.54×10^{-7}	0.46×10^{-3}	<i>Small</i> , 2022 , 18, 2105465
MBFO	4.57×10^{-8}	0.49×10^{-3}	<i>Angew. Chem. Int. Ed.</i> 2021 , 60, 8905
Mn/PSAE	7×10^{-8}	0.11×10^{-3}	<i>Angew. Chem. Int. Ed.</i> 2021 , 60, 9480
LDHzyme	1.41×10^{-6}	3.57×10^{-3}	This work

References

1. M. Sun, Y. Sang, Q. Deng, Z. Liu, J. Ren and X. Qu, *Nano Res.*, 2022, **15**, 5273–5278.
2. Y. Liu, J. Wu, Y. Jin, W. Zhen, Y. Wang, J. Liu, L. Jin, S. Zhang, Y. Zhao, S. Song, Y. Yang and H. Zhang, *Adv. Funct. Mater.*, 2019, **29**, 1904678.
3. Z. Wang, B. Liu, Q. Sun, S. Dong, Y. Kuang, Y. Dong, F. He, S. Gai and P. Yang, *ACS Appl. Mater. Interfaces*, 2020, **12**, 17254–17267.
4. X. Yang, L. Wang, S. Guo, R. Li, F. Tian, S. Guan, S. Zhou and J. Lu, *Adv. Healthc. Mater.*, 2021, **10**, 2100539.
5. L. Wang, L. Zhuang, S. He, F. Tian, X. Yang, S. Guan, G. I. N. Waterhouse and S. Zhou, *ACS Appl. Mater. Interfaces*, 2021, **13**, 59649–59661.